Theor Appl Genet (1989) 77: 295–303

Monoparametric models of flow cytometric karyotypes with spreadsheet software

J. Conia [1], P. Muller [2], S. Brown [2], C. Bergounioux [1] and P. Gadal [1]

[1] Physiologie Végétale Moléculaire, Université de Paris-Sud, bât. 430, F-91405 Orsay Cedex, France
[2] Physiologie Cellulaire Végétale and Service de Cytométrie, CNRS, F-91198 Gif-sur-Yvette Cedex, France

Received April 11, 1988; Accepted August 1, 1988
Communicated by F. Mechelke

Summary. Theoretical flow karyotypes from both plant and mammalian species have been simply modelled using computer spreadsheet software. The models are based upon published values of relative DNA content or relative lengths of each of the chromosomes. From such data, the histograms of chromosome distribution have been simulated for both linear and logarithmic modules of a flow cytometer, and as a function of the coefficient of variation. Simulated and experimental histograms are compard for *Nicotiana plumbaginifolia*. This readily accessible exercise facilitates the planning and execution of flow cytometric analysis and sorting of chromosomes.

Key words: Chromosomes – Flow cytometry – Theoretical flow karyotypes – Spreadsheet software

Introduction

Flow cytometry has emerged as a quantitative technique for the classification of both mammalian and plant chromosomes (Gray and Langlois 1986; Conia and Muller 1988). Flow cytogenetics are based on the analysis of thousands of isolated metaphase chromosomes after their release from the cell and after staining with DNA-specific fluorescent dyes. The chromosomes are passed singly in a fluid stream which is intersected by an intense beam of light, and the fluorescence of the DNA-dye complex is detected by photomultipliers through wave length-specific filters. Flow analysis results in the classification of chromosomes into histograms of their relative fluorescence intensities, depending upon their fluorochrome content. Such histograms are considered typical "flow karyotypes" representative of the species (Gray et al. 1975); flow karyotyping is defined as a quantitative analysis of the relative chromosomal DNA distribution and frequency of a given species. In fact, the stoichiometry between chromosomal DNA and fluorochrome content will depend upon choice and condition of staining (notably, for example, intercalating or base pair-specific stains).

On a flow karyotype, chromosome types are represented as peaks along an abscissa of relative fluorescence intensity. The position of the peak mode is a function of the chromosomal DNA and the peak area is a function of the number of corresponding chromosomes. Two different chromosome types which share similar DNA content may be considered as identical objects on the basis of a single fluorescent parameter and are thus assimilated into a composite peak. Experimentally, such similar chromosome types may often be resolved by bivariate analysis after double staining (Gray et al. 1979; Langlois et al. 1982). Chromosomal modifications such as deletion, addition or translocation modify the DNA content of affected chromosomes and are visualized as changes in mode position or changes in relative peak area (relative frequency). When a peak is well individualized from the others, it has proved possible to sort large quantities (typically several thousands) of the corresponding chromosome type with high purity (Gray et al. 1987). In such flow cytometry, the regular vibrations of the sorting device break the fluid stream into droplets and, by use of an electric field, deflect those containing the chromosome of interest. Sorting chromosomes has proved useful for identification of peaks in flow karyotypes (using microscopy), gene mapping, recombinant DNA library production and in establishing chromosomic addition lines or hybrids.

Offprint requests to J. Conia

It is rare that the chromosomes of a given species are all distinctive on the basis of DNA content. Consequently, flow cytometric analyses not only produce discontinuous chromosome peaks (the most favorable situation), but also composite peaks and shoulders. Interpretation of results is thus more difficult, especially when the chromosomes are not morphologically distinct and microscopic observation of chromosome fractions is inconclusive. Nevertheless, the distribution of the chromosomes can be predicted according to their relative lengths or DNA content, where these have already been established by classical cytology. Such theoretical distributions aid interpretation of the cytometric histogram, indicating the probable position of chromosomes among its various peaks (Grunwald et al. 1983; Grunwald et al. 1986).

In this paper we propose a simple method for obtaining monoparametric models of chromosome distributions using computer spreadsheet software. The frequency distribution of each chromosome is considered to be gaussian, the theoretical flow karyotype (total chromosome distribution) being the sum of these different normal curves. In flow cytometry, the coefficient of variation (CV) is commonly used to evaluate the dispersion arising from both biological and methodological origins: a more robust identification of chromosomes is obtained with a lower CV. This is, therefore, a key variable in the model. Such simulations indicate the degree of resolution among the different chromosome peaks which can be reasonably achieved for a given species (Conia et al. 1987). Moreover, if the aim is to sort one chromosome type, models will indicate the feasible targets and predict the interactions between purity and yield.

Materials and methods

Flow cytometry

The histogram of metaphase chromosomes isolated from *Nicotiana plumbaginifolia* was obtained on an Epics V flow cytometer (Coulter, Florida) after staining with Hoechst 33342 (0.6 μg/ml final concentration). Metaphase chromosomes were isolated from protoplast cultures following the method described in detail for *Petunia hybrida* (Conia et al. 1987). The chromosome isolation buffer was inspired by the procedure proposed for mammalian chromosomes (Van den Engh et al. 1984) and consisted of 5 m*M* Hepes pH 7, 3 m*M* 2-mercaptoethanol, 50 m*M* KC1, 10 m*M* $MgSO_4$ and Triton X-100 (0.25% w/v). Samples of lysed protoplasts were filtered through one layer of Miracloth (Calbiochem-Behring Corp., USA) before being used for flow cytometric analysis.

Computer equipment

The computer spreadsheet software used was VP Planner (Paperback Software Int., USA), on a Tandy 3000 micro-computer 8 MHz (Tandy Corp., USA) with 640 Kb (Kilobyte) RAM (random access memory), a 1.2 Mb (Megabyte) floppy disk and a 20 Mb hard disk.

Principle of the model

Species-specific karyotypes are obtained by ranking metaphase chromosomes. The chromosome classification may be based upon their relative DNA content, using dyes which quantitatively bind to the DNA molecule and subsequently using densitometry (Mendelsohn et al. 1973). However, length is a more common criterion for classification of animal and plant chromosomes, conventionally expressed as the T/θ ratio where T is the absolute length of each chromosome and θ is the total length of the haploid set divided by the number (n) of chromosomes. Our simulations are based upon such published classifications (cited in the legends). The model requires construction of the gaussian frequency distribution for each chromosome type according to its DNA content or relative length, on a 256-channel scale (or as appropriate for the flow cytometer in use), and their summation. Two chromosomes of the same length are handled as a single chromosome with doubled frequency (e.g., as chromosomes 9 and 10 in Fig. 5b).

In reality, amplified fluorescence signals in a range of 0–10 V are converted into a 256-channel scale. We therefore use volts as the units to define the range of each class (channel) in our logarithmic model, where this range is not constant. In the linear model, it is adequate to calculate frequency directly in channel units, the range being constant.

Worksheet layout

Each chromosome or assimilated grouping constitutes a column heading (Table 1), beneath which is entered its relative size (length or DNA content), which will enable calculation of its modal position and standard deviation (SD); this, in turn, is dependent upon the position assigned initially to the largest chromosome and upon the given CV. Each row represents a channel of the parameter used to describe the chromosomes (in 256 classes). Each cell (field defined by the intersection of a column C and row R) contains the frequency for the presence of a chromosome C in the channel R, calculated from a gaussian probability as a function of modal position and SD. A further column is reserved to add the frequencies of the chromosomes across a row. The graphic output of the histogram is automatic: the abscissa is set as channel number and the ordinate as the totalled frequencies of all chromosomes in that channel.

Worksheet size

The capacity to handle more complex karyotypes will be determined by the memory (RAM) available after loading the software. The necessary memory space increases according to the number of different chromosomes and the required resolution (number of channels). The worksheet may typically be created in less than an hour, the calculation time for one simulation varying with the type and size of the worksheet.

To economise memory

Each cell of the table contains a calculation. To decrease calculation time and memory requirement, this formula can be replaced by its result where this is known (namely, when zero). To this end, a simplified simulation is run with only the two extreme chromosomes (with maximal dispersion, or CV) in order to establish the effective range; the unnecessary outlying rows ("channels") of the table are so identified and removed. Likewise, the formula may be replaced by zero in other unnecessary cells. (The new spreadsheet must be saved and re-loaded before the economy of memory is effective.) Decreasing the number of rows frees space for increasing the number of columns (and,

Table 1. An example of the worksheet to simulate flow karyotypes for a linear scale: flow karyotype model for *Petunia hybrida*; CV = 5%, mode of largest chromosome = 200

	A	B	C	D	E	F	G	H
6	Chromosome no.:	1	2	3	4	5 and 6	7	Karyo-
7	Relative length:	**1.20**	**1.03**	**1.02**	**0.97**	**0.94**	**0.89**	type
8	Relative mode:	200.00	171.67	170.00	161.67	156.67	148.33	
9	SD:	10.00	8.58	8.50	8.08	7.83	7.42	
10	Mid-channel	Frequency						
11	0.5	0.00	0.00	0.00	0.00	0.00	0.00	0.00
12	1.5	0.00	0.00	0.00	0.00	0.00	0.00	0.00
13	2.5	0.00	0.00	0.00	0.00	0.00	0.00	0.00
175	164.5	0.01	3.28	3.81	4.64	6.18	0.50	18.41
176	165.5	0.01	3.59	4.08	4.41	5.39	0.37	17.85
177	166.5	0.01	3.88	4.31	4.13	4.63	0.27	17.23
178	167.5	0.02	4.13	4.49	3.80	3.91	0.19	16.56
179	168.5	0.03	4.34	4.62	3.45	3.25	0.13	15.83
180	169.5	0.04	4.50	4.69	3.09	2.66	0.09	15.06
181	170.5	0.05	4.61	4.69	2.72	2.14	0.06	14.26
182	171.5	0.07	4.65	4.62	2.35	1.70	0.04	13.43
183	172.5	0.09	4.63	4.49	2.01	1.32	0.03	12.57
184	173.5	0.12	4.54	4.31	1.69	1.01	0.02	11.69
264	253.5	0.00	0.00	0.00	0.00	0.00	0.00	0.00
265	254.5	0.00	0.00	0.00	0.00	0.00	0.00	0.00
266	255.5	0.00	0.00	0.00	0.00	0.00	0.00	0.00
267	Total	100.00	100.00	100.00	100.00	200.00	100.00	700.00

Given values are shown in bold type

B 008 .. G 008 – Relative mode
C 009 .. G 009 – SD = CV* M
B 011 .. H 270 – Frequency = (N* 100/(SD* SQRT (2* PI)))* EXP(−0.5* ((X-M)/SD) ^ 2)
H 011 .. H 266 – Karyotype = Sum of frequencies of all chromosomes
B 267 .. H 267 – Control = Sum of distributions in all channels for each type of object

CV = Coefficient of variation; SD = Standard deviation; M = Mean (for a normal distribution Mode = Mean); N = Number of chromosomes having this identical length and therefore handled as a single type; X = Channel number; 256 = Number of channels in a given analog-to-digital converter (ADC)

hence, the number of different chromosomes). For example, a table of 15 chromosomes over 256 channels can be replaced by another of 25 chromosomes over 156 useful channels.

Results and discussion

The general worksheet

In its elementary form (Table 1), a worksheet to simulate a karyotype of 16 chromosomes over 256 channels occupied 360 Kb (i.e. saturation of our RAM) and the calculation took 80 s. In principle, model karyotypes could be extended to an unlimited number of chromosomes. Larger karyotypes had to be calculated as such subsets and the overall karyotype was then finally reconstituted from these results and stored in a recapitulative table. Commercial software such as VP Planner provides macrocommands for automatically linking such tables.

Flow karyotype models for different species

Model flow karyotypes are shown for *Homo sapiens* (2n = 46) (Fig. 1 a–c); *Vicia faba* (2n = 12), *Beta vulgaris* (2n = 18) and *Haplopappus gracilis* (2n = 4) (Fig. 2 a–c); *Rattus norvegicus* (2n = 42), *Mus musculus* (2n = 40), *Delphinus delphis* (2n = 44), *Balaenoptera borealis* (2n = 44), *Equus burchelli bohmi* (2n = 44) and *Macaca fascicularis* (2n = 42) (Fig. 3 a–f); and *Sus scrofa domestica* (2n = 38) (male and female Fig. 4 a and b). The CV chosen here was 2%, reasonable for high quality flow cytometry.

The human flow karyotypes simulated either according to the relative DNA content, relative length or base pair number of chromosomes were in agreement with the experimental monoparametric distributions from flow cytometry as described by others (Carrano et al. 1981; Yu et al. 1981). Differences exist between karyotypes, characteristic features distinguishing normal and abnormal individuals: notably, reproducible chromosome polymorphism can be detected (Young et al. 1981). More-

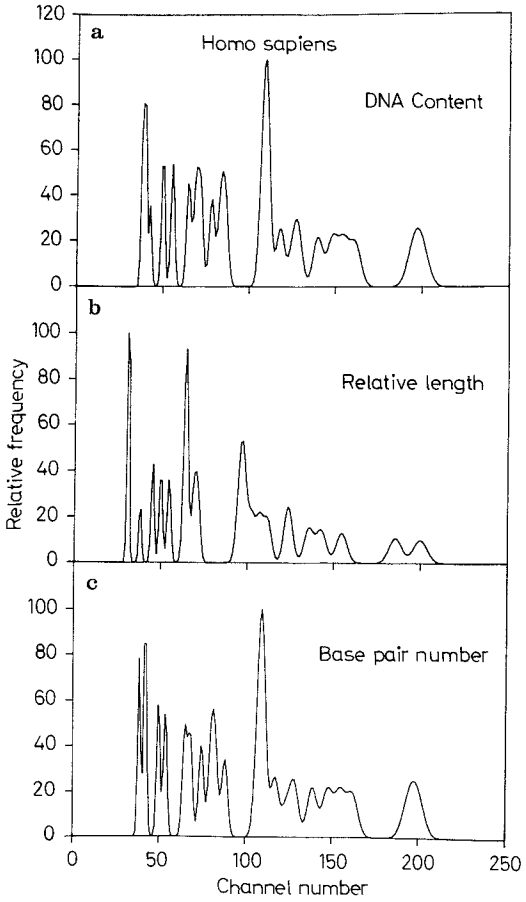

Fig. 1a–c. Model prepared for the 24 human chromosomes (male, one X and one Y) **a** according to the relative DNA content (after Mendelsohn et al. 1973), **b** relative length (after Manolov et al. 1971), and **c** base pair number (after Southern 1982); the simulations were based upon CV = 2%, and the mode of the largest chromosome was set at channel 200

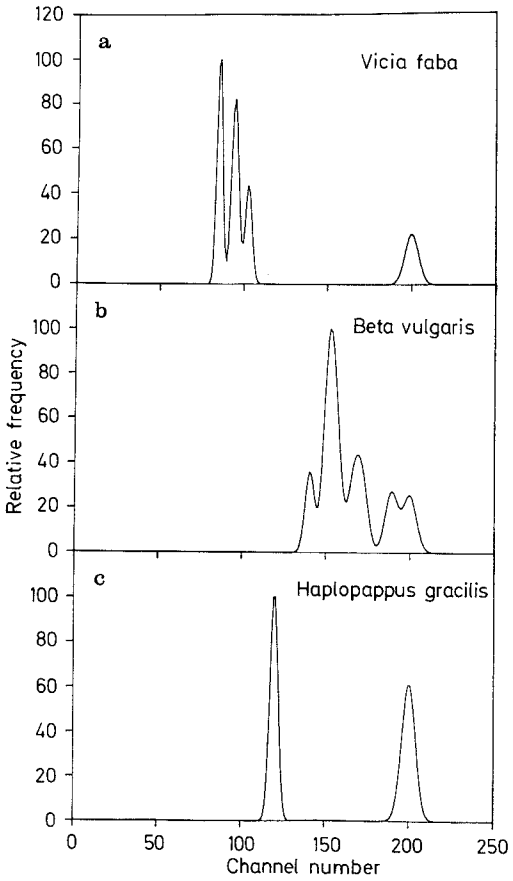

Fig. 2a–c. Model flow karyotypes for different plant species on the basis of a CV = 2%; **a** of the six different chromosomes of the faba bean (after Sjödin 1971), chromosome no. I formed a well-individualized peak (positioned in the model at channel 200); **b** the nine chromosomes of the sugar beet (after Bosemark and Bormotov 1971) were identified as five peaks or shoulders whereas, **c** for the annual Compositae *Haplopappus gracilis* (after Jackson 1957), the two chromosomes of the basic haploid complement were resolved as two separate peaks

over, our three proposed models for the human flow karyotype in Fig. 1 are not identical, as the relative chromosome values for DNA content, length and base pair number differ.

Male and female model flow karyotypes for pig may be compared in Fig. 4. As for experimental histograms (Grunwald et al. 1986), in the simulation, chromosome Y appeared as a well isolated peak.

Flow cytogenetics have only been reported for two plant species: *Haplopappus gracilis* (2n = 4), with two distinctive chromosomes (De Laat and Blaas 1984, and simulated in Fig. 2c) and *Petunia hybrida* (2n = 14), with a less tractable karyotype (experimental and model histograms in Conia et al. 1987). From simulations for *Petunia hybrida* based upon relative chromosome length (Maizonnier 1976), it was evident that because of indistinctive chromosomes, resolution of the flow karyotype and the feasibility to sort designated chromosomes was particularly dependent upon the CV. A model with CV = 2.5% was consistent with the experimental flow karyotype (Conia et al. 1987). When simulated at CV = 1% (as expected with optimal experimental conditions), still only four of the seven different chromosomes could be resolved distinctly. With such material, a two-colour (biparametric) staining methodology is warranted.

Flow karyotyping with *Petunia hybrida* has revealed monochromatid chromosomes (resulting from kinetochore splitting) with half the DNA of the corresponding metaphase form. Consequently, the *Petunia hybrida* flow karyotype was duplicated at half the range of fluorescence intensities observed for the major karyotype (Conia et al. 1987). This occurred also with other plant species such as *Nicotiana plumbaginifolia* (2n = 20) (Fig. 5a) and was confirmed after sorting (data not

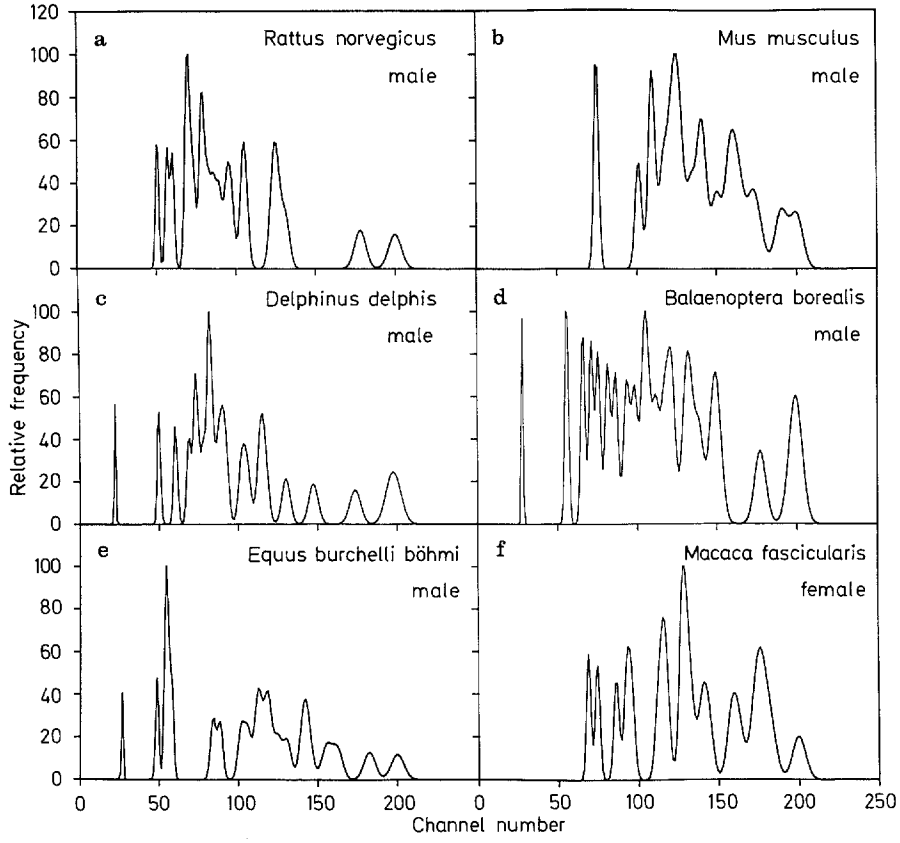

Fig. 3a–f. Model flow karyotypes are shown for different animal species; CV were 2% and the largest chromosomes were positioned at channel 200; theoretical distributions were based upon relative chromosome lengths; from left to right and top to bottom: **a** rat (after Mori and Sasaki 1973), **b** mouse (after Schnedl 1971), **c** common dolphin and **d** sea whale (after Árnason 1974), **e** Böhm's zebra (after Hansen 1975), **f** macaca (after Muleris et al. 1984)

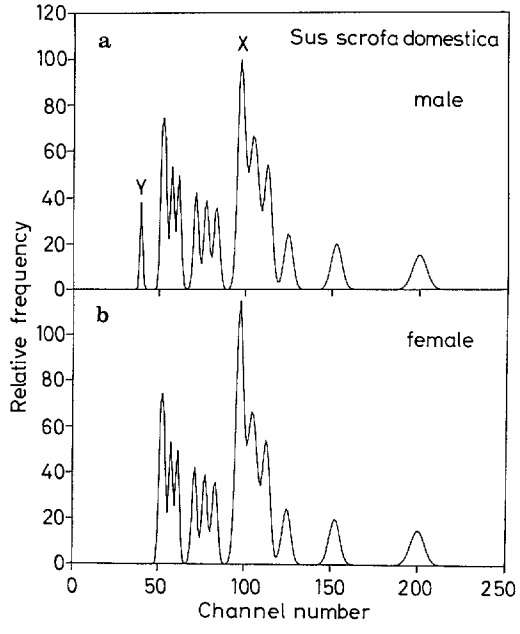

Fig. 4a and b. Model flow karyotypes established for pig, **a** male and **b** female; CV = 2%; porcine chromosomes were after Lin et al. (1980); chromosome Y appeared as an individualized peak and chromosome X, at double frequency, increased the area of the corresponding complex peak

shown); indeed, the upper range of monochromatid forms overlapped the short metaphase chromosomes. Nevertheless, by reference to models based upon relative chromosome length (Fig. 5b), those peaks belonging to the metaphase chromosomes could be distinguished from the duplication resulting from monochromatids. A limitation of the model is evident with chromosomes 1 and 2, which were grouped into a composite but distinctive peak, whereas the experimental distribution proved less distinctive when using Hoechst 33342 as fluorescent ligand (Fig. 5a and b).

Simulation with a logarithmic abscissa

Most cytofluorometers offer logarithmic amplifiers such that fluorescence intensities may be acquired on a logarithmic axis, enabling widely disparate values to be represented on a single scale. The number of decades effective in the conversion module differs between machines (2, 3 or 5 decades, or pseudologarithmic). Using this representation, the karyotype and cell cycle can be depicted on a single histogram. This can be modelled with a simple variation of the initial spreadsheet (Table 2). The frequency of objects is now calculated for a channel whose range (expressed in volts) is variable according to a loga-

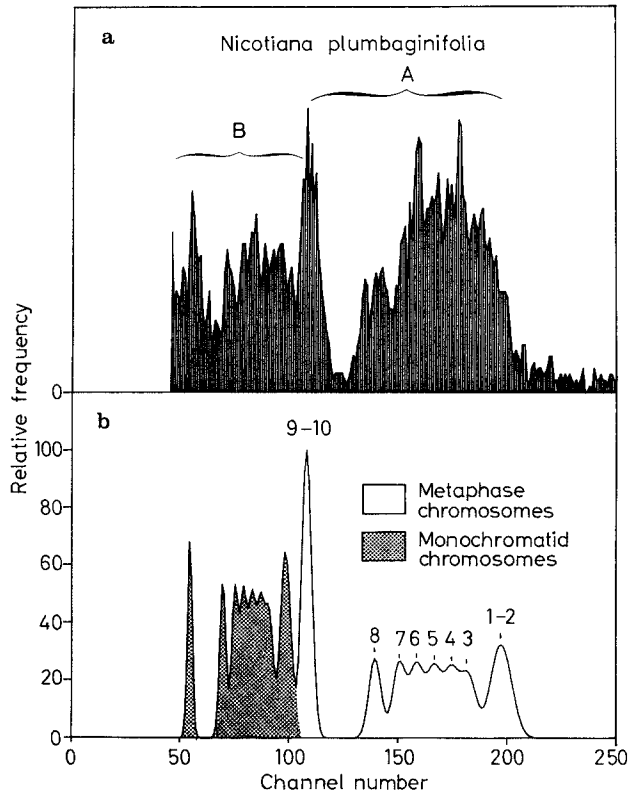

Fig. 5. **a** *Nicotiana plumbaginifolia* experimental flow karyotype (CV about 2.5%); two similar profiles were observed, B having half the fluorescence intensity of A; **b** model flow karyotype with numbering to assign each of the ten chromosomes to its relevant peak (chromosome relative lengths after Mouras et al. 1986); CV = 2%; according to the model, the profile A consisted of metaphase chromosomes while B consisted of monochromatid forms

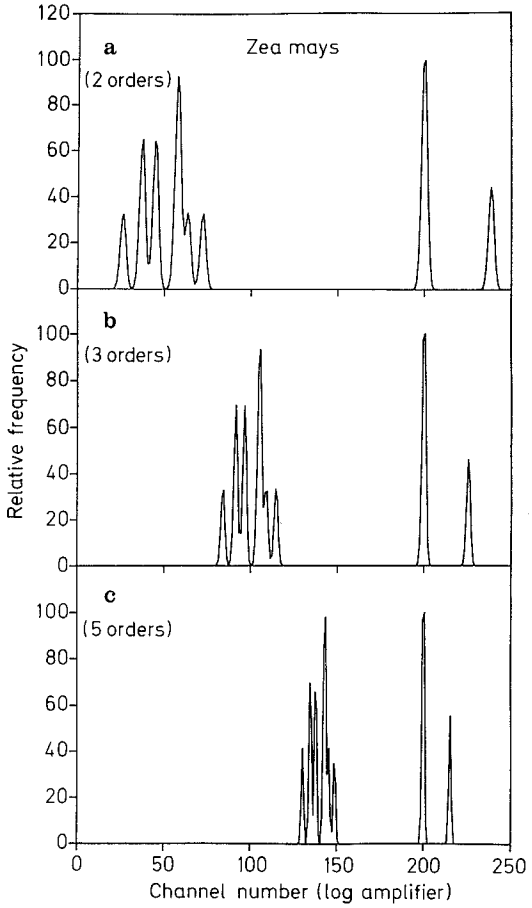

Fig. 6 a–c. Theoretical distribution of the chromosomes and nuclei from maize (2n = 20), models being developed on a logarithmic abscissa (2, 3, 5 decades); chromosome relative lengths were from Sheridan (1982); the mode of the "G0–G1" nuclei was set at channel 200, G2/G0–G1 frequencies and the proportion of nuclei being arbitrary

rithmic function. Notably, this log representation situates the karyotype range relative to the more readily identifiable peaks of nuclei at G0–G1 and G2 in the cell cycle; this facilitates initial experimentation.

From such simulations, the optimal number of decades for the log module can be appreciated (Fig. 6a–c). In a true log function, the distance between any two peaks remains constant and is independent of the position of the karyotype on the axis. To simultaneously visualize chromosomes and nuclei (where extreme values will not differ by more than 100), a log module with two decades would give optimal separation (Fig. 6b). More decades simply compress the range of the karyotype (Fig. 6c).

Conclusion

Monoparametric flow karyotypes may be modelled using commercially available spreadsheet software with a complexity comparable to word processing, and without recourse to programming. This methodology has the virtue of accessibility and simplicity, but at the expense of flexibility and speed relative to a dedicated and compiled program, especially when there are many chromosome types. The simulation produces visual and/or statistical representations of the karyotype. Prior to experimentation, the model reveals the complexity of the analysis, the feasibility of localizing specific chromosomes, the stability (in terms of CV) requisite for resolving different elements and the limitations of a monoparametric analysing. During experimentation, the simulations help work up the flow cytometry (setting scales and gates and identifying zones of interest).

Moreover, when model has the same CV as the experimental histogram, one can evaluate the possible sorting windows and their incidence upon theoretical yield (i.e., for a given chromosome type, the proportion actually within that window) and theoretical purity (frequency of target chromosomes relative to others within the same

Table 2. An example of the worksheet to simulate flow karyotypes for a logarithmic abscissa, flow karyotype model for *Zea mays*, logarithmic scale with variable number of decades

	A	B	C	D	E	F	G	H	I	J	K	L	M
				CV = **5%**		Ploidy = **2**		Intactnuclei = **90%**					
6		Mode G1	(channel) = **200**			Mode G2 = 226		Proportion G2 = **40%**					
7		Mode G1	(volt) = 2.207			Decades = **3**		Proportion S = **20%**					
9	Chromosome no.:			1	2	3	4 and 5	6 and 9	7 and 8	10	G1	G2	Karyo-
10	Length:			**229**	**196**	**179**	**175**	**122**	**140**	**100**	3156	6312	type
11	Mean (Volt):			0.160	0.137	0.125	0.122	0.085	0.098	0.070	2.207	4.413	
12	SD (Volt):			0.008	0.007	0.006	0.006	0.004	0.005	0.003	0.110	0.221	
13	Mid-channel	Midpoint	Lowpoint	**1**	**1**	**1**	**2**	**2**	**2**	**1**	–	–	=N
14		(Volt)	(Volt)	20.00	20.00	20.00	40.00	40.00	40.00	20.00	36.00	36.00	
15	0.5	0.010	0.010	0.00	0.00	0.00	0.00	0.00	0.00	0.00	0.00	0.00	0.00
16	1.5	0.010	0.010	0.00	0.00	0.00	0.00	0.00	0.00	0.00	0.00	0.00	0.00
17	2.5	0.011	0.011	0.00	0.00	0.00	0.00	0.00	0.00	0.00	0.00	0.00	0.00
90	75.5	0.077	0.076	0.00	0.00	0.00	0.00	1.01	0.00	0.72	0.00	0.00	1.73
91	76.5	0.079	0.078	0.00	0.00	0.00	0.00	2.48	0.00	0.19	0.00	0.00	2.68
92	77.5	0.081	0.080	0.00	0.00	0.00	0.00	4.85	0.02	0.03	0.00	0.00	4.90
93	78.5	0.083	0.082	0.00	0.00	0.00	0.00	7.40	0.08	0.00	0.00	0.00	7.48
94	79.5	0.085	0.084	0.00	0.00	0.00	0.00	8.62	0.30	0.00	0.00	0.00	8.92
95	80.5	0.088	0.087	0.00	0.00	0.00	0.00	7.50	0.91	0.00	0.00	0.00	8.41
96	81.5	0.090	0.089	0.00	0.00	0.00	0.00	4.75	2.29	0.00	0.00	0.00	7.03
97	82.5	0.093	0.091	0.00	0.00	0.00	0.00	2.13	4.58	0.00	0.00	0.00	6.72
98	83.5	0.095	0.094	0.00	0.00	0.00	0.00	0.66	7.18	0.00	0.00	0.00	7.84
99	84.5	0.098	0.096	0.00	0.00	0.00	0.00	0.14	8.60	0.00	0.00	0.00	8.74
268	253.5	9.348	9.222	0.00	0.00	0.00	0.00	0.00	0.00	0.00	0.00	0.00	0.00
269	254.5	9.603	9.475	0.00	0.00	0.00	0.00	0.00	0.00	0.00	0.00	0.00	0.00
270	255.5	9.866	9.734	0.00	0.00	0.00	0.00	0.00	0.00	0.00	0.00	0.00	0.00
271	–	–	10.000	–	–	–	–	–	–	–	–	–	–
272	Total			20.00	20.00	20.00	40.00	40.00	40.00	20.00	36.00	36.00	272.01

Given values are shown in bold type

G 006	Position G2 (channel) = position G1 + (256*LOG(2)/DN)
K 010	Equivalent G1 length = ploidy* Sum of length of chromosomes
K 011	Equivalent G2 length = 2* equivalent G1 length
K 014	G1 nuclei = intact nuclei* ((100-%S nuclei -%G2 nuclei)/100)
L 014	G2 nuclei = intact nuclei* % G2 nuclei
D 007	Conversion (channel → volt) = 10 ∧ ((channel* DN/256)-(DN-1))
B 015 .. B 270	Conversion (channel → volt) for midpoint
C 015 .. C 271	Conversion (channel → volt) for lowpoint
D 011 .. L 011	Mean or mode (in volt) = G1 (in volt)* chromosome length/equivalent G1 length
D 012 .. L 012	SD = CV* M
D 014 .. J 014	Number of chromosomes of a type = ploidy* N* (100-% intact nuclei)
D 015 .. L 270	Number of objects of a type in a channel = ((total number of this type/(SD* SQRT(2* PI))* Exp(−0,5* ((midpoint-M)/SD) ∧ 2))* (highpoint-lowpoint)
M 015 .. M 270	Sum of frequencies of all types in a channel
D 272 .. M 272	Control = sum of distributions in all channels for each type of object

CV = Coefficient of variation; SD = Standard deviation; M = Mean (for a normal distribution = Mode); N = No. of chromosomes having this identical length and handled as a single type; DN = No. of decades on the logarithmic amplifier; 256 = No. of channels in a given analog-to-digital converter (ADC)

window). Of course, we cannot address here the machine performance affecting yield and purity. However, having some statistical basis for setting the compromise between yield and purity is all the more necessary when microscopic assessment of sorted samples is impractical due to chromosome similarities. The occurrence of monochromatid chromosomes only serves to underline these advantages when developing flow karyotypes of plant species.

The purpose of our model is simply to convert a quantitative relationship between chromosomes of the haploid set into relative fluorescence intensities and to

introduce statistical dispersion. For human chromosomes (Mendelsohn et al. 1973), the relative DNA content of each chromosome is available, but even here the theoretical flow karyotype will often differ from experimental analysis since the intensity of a stained chromosome may depend upon additional factors. These factors include degree of condensation (e.g. with intercalating fluorochromes such as ethidium bromide) or occurrence of adenine-thymidine rich regions (in the case of Dapi and Hoechst dyes) (Kapuściński and Szer 1979; Weisblum and Haenssler 1974) and cytosine-guanine rich regions (in case of chromomycin A3 and mithramycin) (Fox and Howarth 1985).

More commonly, the relative lengths of chromosomes (T/θ ratio) have been published. Homogeneous condensation throughout the chromosome complement is thus a further assumption of our simulation. Major variation in the degree of condensation of chromatin at metaphase was found in neither animal nor plant organisms with large interspecific differences in C values. Moreover, the total metaphase chromosome volume per cell has been shown to be closely related to the 4 C DNA content of cells with a correlation coefficient of 0.97 (Bennett et al. 1983). Other factors introduce uncertainty in our procedure. Cytological values for a given species published by different sources are not always in agreement; preparative methods, measurement methods, genotype differences, etc., may be the cause. Satellites which are found on chromosomes may introduce discrepancies according to whether or not they were included in the chromosome length, especially as the length of the connection thread may vary. The calculation of length may or may not include the centromeric region.

Powerful analyses and deconvolution of multiple gaussian distributions (with calculation of components of noise and debris) have been undertaken elsewhere and biparametric analyses using two lasers to sequentially excite distinctive fluorochromes (e.g., Hoechst 33258 and chromomycin A3) have proved invaluable in resolving many karyotypes. Our simulation does not address such levels of sophistication; moreover, this would require values for the base composition of each chromosome. Nor has flow karyotyping of plant species, for instance, attained such a level. The merit of our model is its accessibility and simplicity, and its capacity to clarify the options or strategies during the initial development of a flow cytometric study of chromosomes.

References

Árnason Ú (1974) Comparative chromosome studies in Cetacea. Hereditas 77:1–36

Bennett MD, Heslop-Harrison JS, Smith JB, Ward JP (1983) DNA density in mitotic and meiotic metaphase chromosomes of plants and animals. J Cell Sci 63:173–179

Bosemark NO, Bormotov VE (1971) Chromosome morphology in a homozygous line of sugar beet. Hereditas 69:205–212

Carrano AV, Lebo RV, Yu LC, Kan YW (1981) Regional gene mapping of human chromosomes purified by flow sorting. In: Neth R, Gallo RC, Graf T (eds) Modern trends in human leukemia IV. Springer, Berlin Heidelberg New York, pp 156–159

Conia J, Muller P (1988) Isolation, classification and flow cytometric sorting of plant chromosomes. In: Yen A (ed) Flow cytometry: Advanced experimental and clinical applications. CRC Press, Boca Raton/FL, USA (in press)

Conia J, Bergounioux C, Perennes C, Muller P, Brown S, Gadal P (1987) Flow cytometric analysis and sorting of plant chromosomes from *Petunia hybrida* protoplasts. Cytometry 8:500–508

De Laat AMM, Blaas J (1984) Flow-cytometric characterization and sorting of plant chromosomes. Theor Appl Genet 67:463–467

Fox KR, Howarth NR (1985) Investigations into the sequence-selective binding of mithramycin and related ligands to DNA. Nucleic Acids Res 13:8695–8714

Gray JW, Langlois RG (1986) Chromosome classification and purification using flow cytometry and sorting. Annu Rev Biophys Chem 15:195–235

Gray JW, Carrano AV, Steinmetz LL, Van Dilla MA, Moore II DH, Mayall BH, Mendelsohn ML (1975) Chromosome measurement and sorting by flow systems. Proc Natl Acad Sci USA 72:1231–1234

Gray JW, Langlois RG, Carrano AV, Burkhart-Schulte K, Van Dilla MA (1979) High resolution chromosome analysis: One and two parameter flow cytometry. Chromosoma 73:9–27

Gray JW, Dean PN, Fuscoe JC, Peters DC, Trask BJ, Van den Engh GJ, Van Dilla MA (1987) High-speed chromosome sorting. Science 238:323–329

Grunwald D, Reuter W-O, Rosenfeld C, Frelat G (1983) Analyse de chromosomes humains par microcytophotomètre de flux. C R Acad Sci Ser III 297:299–304

Grunwald D, Geffrotin C, Chardon P, Frelat G, Vaiman M (1986) Swine chromosomes: Flow sorting and spot blod hybridization. Cytometry 7:582–588

Hansen KM (1975) The G- and Q-band karyotype of Böhm's or Grant's zebra (*Equus burchelli böhmi*). Hereditas 81:133-140

Jackson RC (1957) New low chromosome number for plants. Science 126:1115–1116

Kapuściński J, Szer W (1979) Interactions of 4', 6-diamidine-2-phenylindole with synthetic polynucleotides. Nucleic Acids Res 6:3519–3534

Langlois RG, Yu LC, Gray JW, Carrano AV (1982) Quantitative karyotyping of human chromosomes by dual beam flow cytometry. Proc Natl Acad Sci USA 79:7876–7880

Lin CC, Biederman BM, Jamro HK, Hawthorne AB, Church RB (1980) Porcine (*Sus scrofa domestica*) chromosome identification and suggested nomenclature. Can J Genet Cytol 22:103–116

Maizonnier D (1976) Etude cytogenetique de variations chromosomiques naturelles ou induites chez *Petunia hybrida* Hort. Thèse Doct ès Sci Nat Université de Dijon, France, pp 1–98

Manolov G, Manolova Y, Levan A (1971) The fluorescence pattern of the human karyotype. Hereditas 69:273–286

Mendelsohn ML, Mayall BH, Bogart E, Moore II DH, Perry BH (1973) DNA content and DNA-based centromeric index of the 24 human chromosomes. Science 179:1126–1129

Mori M, Sasaki M (1973) Fluorescence banding patterns of the rat chromosomes. Chromosoma 40:173–182

Mouras A, Wildenstein C, Salesses G (1986) Analysis of karyotype and C-banding pattern of *Nicotiana plumbaginifolia* using two techniques. Genetica 68:197–202

Muleris M, Paravatou-Petsota M, Dutrillaux B (1984) Diagrammatic representation for chromosomal mutagenesis studies II. Radiation-induced rearrangements in *Macaca fascicularis*. Mutat Res 126:93–103

Schnedl W (1971) The karyotype of the mouse. Chromosoma 35:111–116

Sheridan WF (1982) Maps, Markers and Stocks. In: Sheridan WF (ed) Maize for biological research. III. Genetics and Cytogenetics. A special publication of the Plant Molecular Biology Association. University of North Dakota, University Press, Charlottesville, pp 37–52

Sjödin J (1971) Induced translocation in *Vicia faba* L. Hereditas 68:1–34

Southern EM (1982) Application of DNA analysis to mapping the human genome. Cytogenet Cell Genet 32:52–57

Van den Engh G, Trask B, Cram S, Bartholdi M (1984) Preparation of chromosome suspensions for flow cytometry. Cytometry 5:108–117

Weisblum B, Haenssler E (1974) Fluorometric properties of the bibenzimidazole derivative Hoechst 33258, a fluorescent probe specific for AT concentration in chromosomal DNA. Chromosoma 46:255–260

Young, BD, Ferguson-Smith MA, Sillar R, Boyd E (1981) High-resolution analysis of human peripheral lymphocyte chromosomes by flow cytometry. Proc Natl Acad Sci USA 78:7727–7731

Yu L-C, Aten J, Gray J, Carrano AV (1981) Human chromosome isolation from short-term lymphocyte culture for flow cytometry. Nature 293:154–155